Orbital-free kinetic-energy functionals for first-principles molecular dynamics

Enrico Smargiassi and Paul A. Madden

Physical Chemistry Laboratory, University of Oxford, Oxford OX1 3QZ, United Kingdom
(Received 12 October 1993)

We study a class of kinetic-energy functionals suitable for orbital-free first-principles molecular dynamics and assess their validity for the study of simple metals. With a simple functional which guarantees correct behavior to second order in perturbation theory and approximates higher-order terms, we find that for Na accuracy is already achieved, while Al is reasonably well described. The simple functional can be readily generalized to include higher-order terms.

I. INTRODUCTION

Recently, there has been a considerable effort invested in devising methods based upon the Car-Parrinello (CP) strategy[1] in which the computational effort scales linearly with system size (so-called order-N methods).[2,3] A straightforward implementation of first-principles molecular dynamics (FPMD) with a Kohn-Sham (KS) realization of density-functional theory[4] leads to an algorithm which scales as the cube of the system size, due to the orthogonalization of the KS orbitals. New KS-based schemes have been proposed which do scale linearly. However, these methods depend either upon the possibility of localizing the KS orbitals[2] or upon the finite (short) range of the density matrix,[3] and it therefore does not seem likely that they will be applicable to metals (for which the density matrix elements decay algebraically at long range). We have examined another approach which is based upon the use of an orbital-free density functional in place of the KS scheme.[5]

Leaving aside, for the moment, the difficulties associated with finding a suitable functional for the kinetic energy (which is the subject we take up in this paper), we emphasize the tremendous advantages of formulating FPMD in this way, especially for metals. First, the electronic calculation is formally of order N. Secondly, it is of order N *in practice*, at least for metals, since the calculation can be "conditioned"[5] so that the FPMD time step in the CP scheme does not decrease with increasing system size (equivalently, the number of steps used in finding the electronic ground state does not increase with the system size due to convergence problems when conditioning is applied). An associated benefit is the fact that the ability to perform adiabatic FPMD efficiently does not depend upon the existence of a gap in the spectrum of quasiparticle states, as it does in the KS scheme.[6] Thirdly, since wave functions do not enter the functional, Brillouin-zone sampling is not required to calculate metallic properties accurately.

The Hohenberg-Kohn theorem,[7] cornerstone of the density-functional theory (DFT), guarantees that the electron density alone is sufficient to determine the ground-state properties of the electronic system. In particular, within the Born-Oppenheimer approximation, it determines all the ionic properties of a condensed-matter system. However, direct applications of the theorem to such systems have been scarce to date since no energy functional of sufficient quality has been available. While the exchange-correlation part can be approximated in a surprisingly accurate way with local-density approximation (LDA), the same procedure applied to the kinetic part yields the Thomas-Fermi (TF) functional, which is known to have a number of problems:[8,9] no binding, divergence at the nuclear position, etc. While the use of LDA for exchange correlation, or indeed a total neglect of this term, usually gives only small corrections to the linear-response function (LRF), the same approximation to the kinetic energy gives qualitatively incorrect results: for example, the induced electron density decays exponentially rather than as r^{-3}.[10]

Attempts to improve the TF functional systematically by use of a gradient expansion about the uniform gas do not capture the essential physics for description of condensed-matter systems. The linear-response behavior remains incorrect and for stronger perturbations this expansion, when applied to the calculation of atomic and molecular energies, leads to unsatisfactory results if truncated to the fourth order,[11] and higher-order terms diverge. This is not surprising since the expansion parameters are[12] $s = |\nabla \rho|/\rho^{4/3}$ and $t = |\nabla^2 \rho|/\rho^{1/3}|\nabla \rho|$, which both diverge when exponentially decaying densities are introduced.

The kinetic-energy functionals which we examine here are designed to incorporate several important limiting forms. The uniform limit is represented by the TF functional and the correct behavior of the kinetic energy to second order in density fluctuations about uniform is built in, which guarantees the correct linear response. The large-s limit, important for obtaining converged solutions with pseudopotentials of realistic strength, is handled by including the von Weizsäcker (vW) functional.[13] There are numerous possible functionals which incorporate these limits and we begin by examining the principles on which these functionals are based. Using a quite general form for the second-order functionals, we then assess their validity for FPMD and discuss their shortcomings. For the reasons given above, we focus on simple metals. Finally, we discuss possible improvements and

assess the prospects for the orbital-free methodology as a general approach to metals.

Atomic (Hartree) units will be used throughout the paper, unless otherwise stated.

II. CONSTRUCTION OF THE KINETIC-ENERGY FUNCTIONAL

A. Limiting forms

Although the Hohenberg-Kohn kinetic-energy functional $T[\rho]$ is not known in general, several limiting forms have been established:

(a) For a uniform system,

$$T = T_{\rm TF} = c_k \int d\mathbf{r} \rho^{5/3}(\mathbf{r}), \qquad (2.1)$$

where $c_k = \frac{3}{10}(3\pi^2)^{2/3}$.

(b) For a slowly varying perturbation, the gradient expansion,

$$T_{\rm GE} = T_{\rm GE}^{(0)} + T_{\rm GE}^{(2)} + \cdots$$
$$= T_{\rm TF} + \frac{1}{72} \int d\mathbf{r}|\nabla\rho|^2/\rho + \cdots. \qquad (2.2)$$

(c) For a rapidly varying perturbation, the von Weizsäcker functional,[13]

$$T_{\rm vW} = \frac{1}{2}\int d\mathbf{r} \rho^{\frac{1}{2}}\nabla^2\rho^{\frac{1}{2}} = \frac{1}{8}\int d\mathbf{r}|\nabla\rho|^2/\rho = 9T_{\rm GE}^{(2)}. \quad (2.3)$$

(The second equality, although not true in general, is valid in the practical cases of vanishing or periodic boundary conditions.) It is believed[9] that $T_{\rm vW}$ is the asymptotic behavior of T in the case of rapidly varying densities, $T_{\rm TF}$ being the lowest-order correction. The $T_{\rm vW}$ functional, moreover, is exact for the ground state of a system with one or two electrons, or in which the one-electron wave functions do not overlap.

(d) For small perturbations, the correct form is obtained from linear-response theory (LRT).[7] This implies

$$\delta^2 T/\delta\rho^2\big|_{\rho_0} = -1/\chi_0, \qquad (2.4)$$

where $\delta/\delta\rho$ is the functional derivative, ρ_0 is the average electron density, and χ_0 is the LRF of the noninteracting homogeneous electron gas, i.e. the Lindhard function.[10] It is important to notice that it is this term that gives rise to the celebrated Friedel oscillations, which are an essential feature of any description of metals.[10]

B. Earlier work

In the past, several attempts have been made to use one or another of these forms for atomic, molecular, or solid systems. The validity of the gradient expansion up to the fourth order for molecular binding has been examined by Perdew et al.[11] and found wanting in this case. On the other hand, $T_{\rm vW}$ has been used fairly success-

fully to compute lattice parameters and bulk moduli in simple metals[14] and has been used in the calculation of embedded-atom potentials.[15] Many authors have tried to improve upon the simple second-order gradient expansion and the vW functional by using some interpolation between the two, either by writing simply[16,17] $T = \frac{\lambda}{8}\int d\mathbf{r}|\nabla\rho|^2/\rho$, $\lambda \in [\frac{1}{9},1]$, or using Padé approximants.[9] In all cases the interpolation parameters were determined by a suitable fit to other data, such as Hartree-Fock atomic energies. Analogous expressions were obtained via semiclassical expansions.[9]

A common problem to all these approaches is that they do not satisfy Eq. (2.4), and hence they do not give Friedel oscillations. This is most easily seen by linearizing the kinetic-energy functional and taking its Fourier transform.[18] They approximate the exact linearized kinetic-energy kernel but do not have the tiny but all-important singularity at $2k_f$. For example, nth-order gradient expansion gives an nth-order polynomial.

C. A family of kinetic-energy functionals

Our aim is to construct a kinetic-energy functional which incorporates the largest possible number of exact limits, in the hope that it turns out to interpolate well between them. This approach has been suggested by several workers. We write a general trial functional which embodies most of these suggestions as follows:

$$T_\alpha[\rho] = T_{\rm TF} + T_{\rm vW}$$
$$+ \int\int d\mathbf{r}\,d\mathbf{r}'\Delta\rho^\alpha(\mathbf{r})K_\alpha(\mathbf{r}-\mathbf{r}')\Delta\rho^\alpha(\mathbf{r}'), \qquad (2.5)$$

where $\Delta\rho = \rho - \rho_0$ and $\alpha > 0$ is a parameter. This functional satisfies, at least asymptotically, the limiting conditions (a) and (c). If K_α is chosen such as to satisfy Eq. (2.4) and $\langle K_\alpha(\mathbf{r})\rangle = 0$, the limit (d) is also satisfied. This is equivalent to saying that, in reciprocal space,

$$K_\alpha(G) = -\frac{1/\chi_0 - 1/\chi_{\rm vW} - 1/\chi_{\rm TF}}{2\alpha^2\Omega\rho_0^{2(\alpha-1)}}, \qquad (2.6)$$

Ω being the system volume (whose appearance here is due to our definitions of Fourier transforms), $\chi_{\rm TF} = -k_f/\pi^2$ the Thomas-Fermi LRF, and $\chi_{\rm vW} = -4k_f^3/3\pi^2 G^2$ the von Weizsäcker LRF.

Functionals of this kind (or equivalent) have been proposed with $\alpha = 1$ (Ref. 19) and $\alpha = 5/6$ (Ref. 20). Another possibility is $\alpha = 1/2$; with this choice it is possible to satisfy also condition (b), since in this case the long-wavelength components of the kinetic-energy functional must obey the gradient expansion in the linear regime. This is akin to the approaches quoted above[9,16,17] but in this case the exact LRT is retained. In this sense, it is the optimal approach of this kind in metals.

Recently, Perrot[19] proposed a slightly different form:

$$T_P[\rho] = T_{\rm TF} + T_{\rm vW}$$
$$+ \int\int d\mathbf{r}\,d\mathbf{r}'P(\mathbf{r})K_\alpha(\mathbf{r}-\mathbf{r}')P(\mathbf{r}'), \qquad (2.7)$$

where $P(\mathbf{r}) = \frac{6}{5}\frac{\rho_0 + \nu\Delta\rho}{\rho}(\rho^{5/6} - \rho_0^{5/6})$ and $\nu = \frac{5}{\sqrt{32}}$. This form has the correct scaling for $\rho_0 \to 0$ and hence it should be more suited for low-density systems.

Chacón et al. (CAT)[21] have proposed yet another form:

$$T_{\text{CAT}} = \frac{8}{5}c_k \int d\mathbf{r}\,\rho(\mathbf{r})\bar{\rho}^{2/3}(\mathbf{r})$$

$$-\frac{3}{5}c_k \int d\mathbf{r}\,\rho^{5/3}(\mathbf{r}) + T_{\text{vW}}[\rho], \qquad (2.8)$$

$$\bar{\rho}(\mathbf{r}) = \int d\mathbf{r}'\tau(|\mathbf{r} - \mathbf{r}'|, \rho(\mathbf{r}))\rho(\mathbf{r}'), \qquad (2.9)$$

where τ is chosen such as to satisfy Eq. (2.4). This form presents a few technical problems of its own, but is otherwise based on the same physical principles as Eq. (2.5), especially when $\alpha = 5/6$. As we shall see, there are substantial reasons to believe that the specific form in which limits (a)–(d) are implemented makes no real difference in the physical results; therefore T_{CAT} will not be explicitly studied in the present work.

The above functionals all incorporate exact linear response and the correct uniform and large-s behavior. Where they differ is in their implicit representation of the higher-order response functions and it is this property which we examine in the present work. In an important paper, Wang and Teter[20] have discussed how functionals of the chosen general form could be extended to guarantee correct results at the third order of perturbation theory. We will return to a discussion of their findings in the final section.

III. RESULTS FOR SIMPLE METALS

Since our target problems are simple metals we discuss in this section a comparison of the results obtained with various kinetic-energy functionals which fit into the general scheme with experimental results and with Kohn-Sham calculations on sodium and aluminum. The kinetic-energy functionals are combined with the standard Coulomb (Hartree) and Ceperley-Alder exchange-correlation functionals[22] and with local pseudopotentials which have already been examined in Kohn-Sham calculations. The kinetic-energy functionals are distinguished by the parameter α, and we choose T_1 (Perrot), $T_{5/6}$ (Wang-Teter), and $T_{1/2}$. In order to illustrate the contribution of higher-order terms in perturbation theory, we

also give results obtained from linear response theory— note that this LRT result involves linearization of the exchange-correlation functional as well as linearization of the kinetic-energy functional. The comparison with LRT is also significant because the effective pair potentials which are normally used in simulation of metals are derived by an application of linear-response theory to a suitably chosen pseudopotential.[23] Thus our work only represents an advance over this effective potential approach if we can demonstrate that good results can be obtained with transferable pseudopotentials which are so strong as to be outside the linear domain.

A. Sodium

In Table I we compare the calculated values of several physical properties of sodium using different functionals. All results have been obtained using a Topp-Hopfield pseudopotential[24] which is a local, norm-conserving potential which correctly reproduces the lowest excitation energy of the isolated atom in a Hartree-Fock calculation. We use a plane-wave cutoff of 11 Ry, which gives an excellent convergence for all of our functionals. Our formation and migration energies for the vacancy were calculated with a 128-atom cell (which gives convergence within 0.01 eV).

We see from the table that the lattice parameter, bulk modulus, and vacancy-formation energy for T_1, $T_{5/6}$, and $T_{1/2}$ are obtained with a precision similar to that of state-of-the-art KS calculations[25] and experiment. The Kohn-Sham results were obtained with a 54-atom cell and extensive Brillouin-zone sampling (corresponding to 112 k points in a single-atom unit cell).

The results for T_1, $T_{5/6}$, and $T_{1/2}$ are similar to each other. They are also quite similar to the results obtained with LRT; this supports the idea that sodium can be reasonably well described by pair potentials. We also include in the table results obtained with the modified Perrot functional T_P, Eq. (2.7); these are similar to the T_1 results as would be expected for the electron density ($r_s = 3.93$) in sodium. These results should also be compared with previous calculations using the von Weizsäcker functional (Ref. 14: $B = 0.0805$ Mb) or a generalized Weizsäcker functional (Ref. 16: $B = 0.072$ Mb, $a = 7.80$ a.u.).

The phonon dispersion curves of Na have been previously calculated using the T_1 functional;[5] $T_{1/2}$ and $T_{5/6}$ do not give significantly different results. One might con-

TABLE I. Calculated physical properties of Na compared with experimental results. a_{lat}: lattice parameter (a.u.). B: bulk modulus (Mbar). E_f^u: formation energy of the ideal vacancy (eV). E_f^r: formation energy of the relaxed vacancy (eV). E_m: migration energy of the vacancy (eV). KS results from Ref. 25. Experimental results from Ref. 30.

	$T_{1/2}$	$T_{5/6}$	T_1	T_P	LRT	KS	Expt.
a_{lat}	8.11	8.14	8.14	8.11	8.04	7.65	7.98
B	0.069	0.065	0.065	0.061	0.072	0.091	0.064–0.079
E_f^u	0.45	0.50	0.52		0.50	0.45	–
E_f^r	0.36	0.37	0.37		0.40	0.36	0.35
E_m	0.05	0.13	0.03		0.06		0.03

sider this trivial, since in sodium LRT seems to work. However, we found that straightforward LRT gives a systematic overestimation of the phonon frequencies by about 10% (this is in agreement with the original findings of Topp and Hopfield[24]). To solve the apparent paradox, one has to realize that pseudopotentials used in *ab initio* calculations, like Topp and Hopfield's, are usually chosen to be norm conserving to ensure maximum transferability. By contrast, pseudopotentials constructed for use within LRT with the aim of deriving effective pair potentials are optimized so as to have the smallest possible amplitude.[23] Therefore, if one uses a pair potential constructed in that way one obtains excellent results for the phonons; however, this is not a guarantee that if the same pseudopotential is used in a different environment, like the one surrounding a defect, results of similar quality will be obtained.

B. Aluminum

For aluminum (Table II) we used a local pseudopotential due to Goodwin *et al.*,[26] which has been extensively used in Kohn-Sham calculations. We found the Goodwin *et al.* potential to require a plane-wave cutoff of 28 Ry for convergence with our functionals (as manifested by converged forces). Aluminum provides a much sterner test of the orbital-free functionals than sodium, as its pseudopotential is considerably stronger. In fact, we find that, at variance with sodium where the density just manages to stay positive everywhere within LRT (but becomes negative if the full nonlinear exchange-correlation term is included), in aluminum it becomes strongly (of the order $-\rho_0$) negative inside the ionic core. Although the core region is believed to be unimportant for the chemical bond, such a negative density does not bode well for the transferability of effective interatomic potentials or for the calculation of cohesive energies and similar quantities.

1. Structural energies

For aluminum it is possible to make an extensive comparison with Kohn-Sham results with a local pseudopotential that are well converged with respect to Brillouin-zone sampling, since Robertson *et al.*[27] have recently presented an extensive compilation of total energies for a wide variety of crystal structures. This comparison is shown in Table III. We see from the first line that the orbital-free functional gives an excellent value for the energy of the stable crystal (fcc). To demonstrate that this

TABLE II. As in Table I, for Al. LRT, KS, and experimental data from Refs. 26 and 28.

	$T_{1/2}$	$T_{5/6}$	T_1	LRT	KS	Expt.
a_{lat}	7.49	7.63	7.67	6.72	7.60	7.64
B	0.69	0.72	0.70	1.44	0.79	0.74
E_f^v	0.21	1.38	1.63	-0.26	0.64	

TABLE III. Calculated total energy for fcc Al (top row), and energy differences with respect to the fcc structure (lower rows). KS data from Ref. 27. VL stands for vacancy lattice (one atom out of four missing); sc for simple cubic; DIA for diamond). Energies in eV.

	$T_{1/2}$	$T_{5/6}$	T_1	LRT	KS
fcc	-58.43	-58.33	-58.30	-59.08	-58.31
bcc	0.13	0.07	0.06	0.34	0.07
VL	0.21	0.36	0.37	0.71	0.21
sc	0.28	0.34	0.33	0.88	0.40
DIA	0.77	0.80	0.53	1.98	0.89

agreement is not an accident and is the result of a correct account of higher-order perturbation effects we make use of an analysis suggested by Gillan[28] which exposes the importance of the higher-order terms. We perform a series of calculations for the crystal energy in which the pseudopotential is scaled by a factor C which varies from 0 to 1. From a perturbation analysis we expect

$$E(C) = E^{(0)} + C^2 E^{(2)} + C^3 E^{(3)} + \cdots, \quad (3.1)$$

where $E^{(0)}$ is the energy of the uniform electron gas of density ρ_0 plus the Madelung energy of the ions, and the second-order energy $E^{(2)}$ is that associated with the linear response. Both these terms are given correctly by construction in our calculations. In Fig. 1 we plot

$$\Delta E(C) = [E(C) - E(0)]/NC^2 \quad (3.2)$$

[N being the number of atomic sites and $E(C) - E(0)$ the so-called electronic relaxation energy] versus C. The $C = 0$ intercept is therefore $E^{(2)}$, the slope at $C = 0$ is $E^{(3)}$, etc. Our results for $\Delta E(C)$ are compared with those obtain by Gillan[28] from KS calculations with the same pseudopotential on a 27-atom cell. The straight line shows his calculation of the third-order perturbation result. It can be seen that the orbital-free results reproduce the KS ones very well over the whole range of C, at least for the fcc crystal, and that the third-order result is a reasonable tangent to these curves for small C.
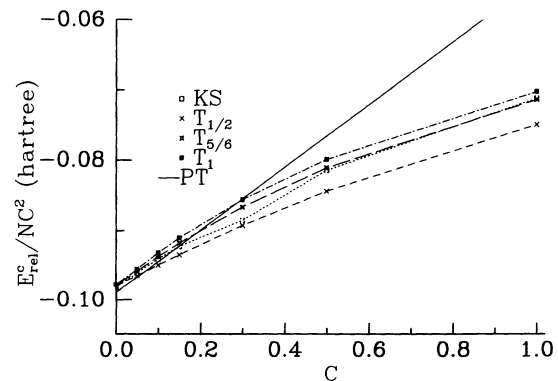
The lower lines in Table III show the energy of other

FIG. 1. Electronic relaxation energy per atom for the Al crystal vs scaling parameter C. Third-order perturbation theory (PT) and KS results are for a $N = 27$ atom cell (after Gillan, Ref. 28).

crystal lattices and the differences from the fcc structure. It can be seen that the discrepancies with the KS results become more pronounced as the lattice becomes more open; the energy difference between bcc and fcc is satisfactory but for the diamond and vacancy lattices it is poorer. This indicates that the ability of functionals of the form of Eq. (2.5) to represent the higher-order perturbation terms is not constant and depends on the coordination structure. It is also clear that the discrepancies differ for the different kinetic-energy functionals; we will discuss this point further below.

2. Vacancy

This pattern is also evident in comparison between experimental quantities and our calculations. The lattice parameter and bulk modulus, which are properties of the perfect fcc lattice, are reproduced well by the orbital-free functionals, but the vacancy-formation energy is poor. Note that for aluminum these quantities are well outside the domain of linear response theory. The disagreement with experiment in the vacancy-formation energy is not a consequence of using a local pseudopotential since Gillan[28] has obtained a good value for the vacancy-formation energy in KS calculations with the same pseudopotential.

As with the total energy, we can analyze the contributions of different orders of perturbation theory by performing calculations with a scaled pseudopotential. The (unrelaxed) vacancy-formation energy $E_V^f(C)$ is given by

$$E_f^u(C) = E(N - 1, V(N - 1)/N, C)$$
$$- \frac{N - 1}{N} E(N, V, C), \qquad (3.3)$$

where $E(N, V, C)$ is the energy of a system of N atoms in volume V with pseudopotential scaling parameter C. Again, in Fig. 2 we can compare values of

$$\Delta E_f^u(C) = [E_f^u(C) - E_f^u(0)]/C^2 \qquad (3.4)$$

with the KS results of Gillan for the same quantity and

with the prediction of third-order perturbation theory, which is the straight line. The perturbation result is for the 27-atom cell which was used in the KS calculations but it does not differ greatly from the infinite-system value. The significant thing about this plot for our general development is that it shows that the failure of the orbital-free density functionals to give the correct vacancy-formation energy in aluminum is primarily due to a failure to represent the third-order perturbation results correctly.

The finding that there are important third-order contributions to the vacancy in aluminium is also known from effective-potential studies. Jacucci et al.[29] showed that effective pair potentials gave poor values and that a substantial improvement could be brought about by including a three-body potential derived from third-order perturbation theory.

The figure shows up significant differences between the different kinetic-energy functionals in their representation of the higher-order terms. It would appear that the $T_{1/2}$ functional is performing better than T_1 and $T_{5/6}$. However, this improvement is not so great as to lead to good vacancy properties and our general conclusion is that an explicit representation of the third-order term needs to be added for a successful description of this defect in aluminum. The heartening thing about the comparison of the different functionals is that they agree with each other and with the KS results about the magnitude of the contributions from beyond third order. If these results were "corrected" by substituting the exact third-order term for the linear term in the expansion of $\Delta E_f^u(C)$ the resulting vacancy-formation energy would be within the range of experimental uncertainty. This gives the hope that the higher-order terms are well represented by the nonlinear terms arising from the von Weizsäcker and Thomas-Fermi functionals for problems of this type.

3. Phonons

We complete the comparison with experimental results for aluminum by showing the calculated (for technical details see Ref. 5) and observed phonon dispersion curves in Fig. 3. The values from $T_{5/6}$ are not shown since
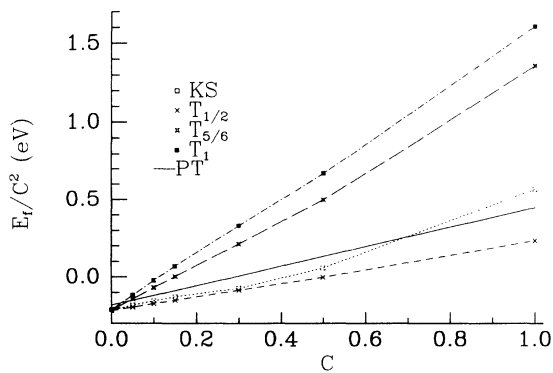

FIG. 2. Formation energy of the Al vacancy as a function of the pseudopotential scaling parameter C. A 32-atom cell was used, except for the PT and KS results,[28] which were obtained using a 27-atom cell.
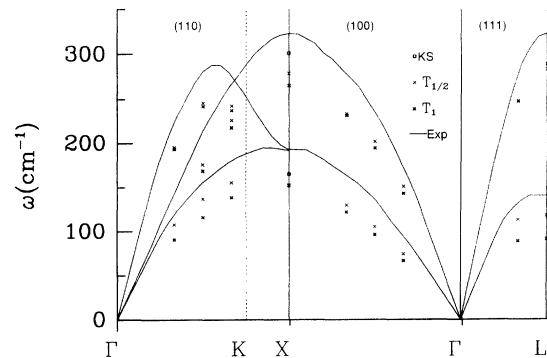

FIG. 3. Phonon dispersion curves for Al at 75 K, as calculated using orbital-free FPMD (crosses). Experimental data (lines) from Ref. 30; KS values (squares) from Ref. 26.

they always lie in between T_1 and $T_{1/2}$. The orbital-free DFT results give systematically low phonon frequencies throughout the Brillouin zone. The overall error on the frequencies is about 10–20%. However, as can be seen from the KS results at the X point using the same pseudopotential,[26] much of this discrepancy is due to the pseudopotential and maybe LDA, rather than to the kinetic-energy functional itself.

IV. DISCUSSION

This work was motivated by the desire to find an *ab initio* order-N method for FPMD which works for simple metals at the level of accuracy of Kohn-Sham calculations and with the same degree of transferability. We have shown that the orbital-free DFT-based method is very promising in this regard. It already gives an excellent account of sodium at a small fraction of the computational cost of KS calculations which agree with experiment. Furthermore, we have demonstrated that with inclusion of a direct representation of the third-order perturbation terms we will achieve a similarly good account of aluminum, including the vacancy. Borrowing from the work of Wang and Teter[20] we know that this can be achieved without negating the advantages of the orbital-free scheme, and work is in progress to implement these terms. At this level, we believe that the technique will become the method of choice for simulating a range of metallic systems. Still more ambitious targets might be achievable: Wang and Teter[20] have already shown that, with inclusion of the third-order term, an orbital-free functional gives a very good account of the electron density in silicon. One potential limitation of the method is that, as presently formulated, only local pseudopotentials may be used. However, recent work on Green's function Monte Carlo methods has shown how nonlocality may be represented without wave functions and it may well be that similar methods could be employed here.[31]

A simpler alternative to even an order-N FPMD method for simple metals is to perform classical simulations with effective interion potentials.[23] The principal advantage which the *ab initio* approach should confer over this procedure is a higher degree of transferability. Effective potentials are constructed from pseudopotentials which are parametrized to minimize the importance of higher-order terms (of higher order than linear response if pair potentials are used). Since the real electron-ion interactions are outside the linear response régime (even for sodium, as evidenced by the behavior of the phonons calculated with the Topp and Hopfield potential), this parametrization must depend upon the electron density and the effective potentials are inconsistent if used in problems where the density takes a different value. The orbital-free DFT approach incorporates the nonlinearity in both the kinetic and exchange-correlation functionals. The kinetic-energy functionals we have discussed here rely on the von Weizsäcker and Thomas-Fermi functionals to play this role but, as we have stressed, a more accurate representation will be developed. The nonlinearity in the exchange-correlation enters directly, through the use of an appropriate functional, and also indirectly through the use of pseudopotentials calculated with a nonlinear core correction;[32] we have already developed the nonlinear core correction in the orbital-free framework. The local spin-density formalism[18] and gradient correction to the LDA[33] are easily implementable too. Finally, we remark that the use of a first-principles scheme gives at any step the electronic density of the system under study consistently with the ionic positions and "for free."

ACKNOWLEDGMENTS

[1] R. Car and M. Parrinello, Phys. Rev. Lett. **55**, 2471 (1985).

[2] G. Galli and M. Parrinello, Phys. Rev. Lett. **69**, 3547 (1992).

[3] S. Baroni and P. Giannozzi, Europhys. Lett. **17**, 547 (1992); X. P. Li, W. Nunes, and D. Vanderbilt, Phys. Rev. B **47**, 10 891 (1993).

[4] W. Kohn and L. J. Sham, Phys. Rev. **140**, A1133 (1965).

[5] M. Pearson, E. Smargiassi, and P. A. Madden, J. Phys. Condens. Matter **5**, 3321 (1993).

[6] G. Pastore, E. Smargiassi, and F. Buda, Phys. Rev. A **44**, 6334 (1991).

[7] P. Hohenberg and W. Kohn, Phys. Rev. **136**, B864 (1964).

[8] R. G. Parr and W. Yang, *Density Functional Theory of Atoms and Molecules* (O.U.P., Oxford, 1989).

[9] R. M. Dreizler and E. K. U. Gross, *Density Functional Theory* (Springer-Verlag, Berlin, 1990).

[10] N. W. Ashcroft and N. D. Mermin, *Solid State Physics* (Saunders, Philadelphia, 1976); W. A. Harrison, *Solid State Theory* (McGraw-Hill, New York, 1970).

[11] J. P. Perdew, M. Levy, G. S. Painter, S. Wei, and J. B. Lagowski, Phys. Rev. B **37**, 838 (1988).

[12] V. Sahni, J. Gruenebaum, and J. P. Perdew, Phys. Rev. B **26**, 4371 (1982).

[13] C. F. von Weizsäcker, Z. Phys. **96**, 431 (1935).

[14] J. M. López, M. P. Iniguez, and J. A. Alonso, Phys. Status Solidi B **100**, 701 (1980).

[15] M. S. Daw, Phys. Rev. B **39**, 7441 (1989).

[16] J. R. Chelikowski, Phys. Rev. B **21**, 3074 (1980).

[17] M. L. Plumer and M. J. Stott, J. Phys. C **18**, 4143 (1985).

[18] R. O. Jones and O. Gunnarson, Rev. Mod. Phys. **61**, 689 (1989).

[19] F. Perrot (unpublished).

[20] L.-W. Wang and M. P. Teter, Phys. Rev. B **45**, 13196 (1992).

[21] E. Chacón, J. E. Alvarellos, and P. Tarazona, Phys. Rev. B **32**, 7868 (1985).

[22] D. M. Ceperley and B. J. Alder, Phys. Rev. Lett. **45**, 566 (1980); J. P. Perdew and A. Zunger, Phys. Rev. B **23**, 5048

(1981).

[23] J. Hafner, *From Hamiltonians to Phase Diagrams* (Springer-Verlag, Berlin, 1987).

[24] W. C. Topp and J. J. Hopfield, Phys. Rev. B **7**, 1295 (1973).

[25] U. Breier, W. Frank, C. Elsässer, and M. Fähnle (unpublished).

[26] L. Goodwin, R. J. Needs, and V. Heine, J. Phys. Condens. Matter **2**, 351 (1990).

[27] I. J. Robertson, V. Heine, and M. C. Payne, Phys. Rev. Lett. **70**, 1944 (1993).

[28] M. J. Gillan, J. Phys. Condens. Matter **1**, 689 (1989).

[29] G. Jacucci, R. Taylor, A. Tenenbaum, and N. van Doan, J. Phys. F **11**, 793 (1981).

[30] *Numerical Data and Functional Relationships in Science and Technology*, Landolt-Börnstein (Springer-Verlag, Berlin, 1991).

[31] G. B. Bachelet, D. M. Ceperley, and M. G. B. Chiocchetti, Phys. Rev. Lett. **62**, 2088 (1989).

[32] G. E. Engel and R. J. Needs, Phys. Rev. B **41**, 7876 (1990).

[33] J. P. Perdew and Wang Yue, Phys. Rev. B **33**, 8800 (1986); A. D. Becke, Phys. Rev. A **38**, 3098 (1988).